

Electro-osmotic flows inside triangular microchannels

This content has been downloaded from IOPscience. Please scroll down to see the full text.

2014 J. Phys.: Conf. Ser. 501 012026

(<http://iopscience.iop.org/1742-6596/501/1/012026>)

View [the table of contents for this issue](#), or go to the [journal homepage](#) for more

Download details:

IP Address: 78.189.45.240

This content was downloaded on 25/06/2016 at 11:29

Please note that [terms and conditions apply](#).

Electro-osmotic flows inside triangular microchannels

P Vocale^{*1}, M Geri², GL Morini² and M Spiga¹

¹Department of Industrial Engineering, University of Parma, Parco Area delle Scienze 181/A, 43124 Parma, Italy.

²DIN, Alma Mater Studiorum Università di Bologna, Viale Risorgimento 2, 40136 Bologna, Italy.

E-mail: pamela.vocale@unipr.it; michela.geri@unibo.it; gianluca.morini3@unibo.it; marco.spiga@unipr.it.

Abstract. This work presents a numerical investigation of both pure electro-osmotic and combined electro-osmotic/pressure-driven flows inside triangular microchannels. A finite element analysis has been adopted to solve the governing equations for the electric potential and the velocity field, accounting for a finite thickness of the electric double layer. The influence of non-dimensional parameters such as the aspect ratio of the cross-section, the electrokinetic diameter and the ratio of the pressure force to the electric force on the flow behavior has been investigated. Numerical results point out that the velocity field is significantly influenced by the aspect ratio of the cross section and the electrokinetic diameter. More specifically, the aspect ratio plays an important role in determining the maximum volumetric flow rate, while the electrokinetic diameter is crucial to establishing the range of pressures that may be sustained by the electro-osmotic flow. Numerical results are also compared with two correlations available in the literature which enable to assess the volumetric flow rate and the pressure head for microchannels featuring a rectangular, a trapezoidal or an elliptical cross-section.

1. Introduction

The progress of lab-on-a-chip technology has allowed an unprecedented development of several fields, both in fundamental and applied research. Microfluidic systems enable systematic, high-throughput manipulation of different classical as well as biological fluids in integrated systems that are designed to perform a number of different operations at ones. A crucial issue for these miniaturized experimental platforms is high-precision fluid transport control. Electro-osmotic pumps (EOPs) can easily achieve such task while working with several fluids, and because there are no moving parts, they do not suffer from manufacturing as well as maintenance issues, like mechanical pumps.

Electro-osmosis is a surface electro-kinetic effect that can arise at the interface between a solid and a liquid. It has been proved to be effective in fluid pumping whenever the system has at least one dimension in the micro- or nano-scale. Most materials obtain a surface electric charge when in contact with a polar medium. The surface charge induces a re-distribution of ions in the electrolyte, generating

*¹ To whom any correspondence should be addressed.



what is known as the Electric Double Layer (EDL). When an electric field is applied, the excess counterions in the EDL move under the applied electric force, pulling the liquid with them. Such movement is then conveyed to the fluid bulk by viscous forces, resulting in an Electro-Osmotic Flow (EOF).

The microchannel cross-sectional geometry plays an important role in defining the flow behaviour, since the local net charge density in the EDL significantly influences the electro-osmotic flows. The dynamic behavior of EOFs through simple geometries, such as circular tubes or parallel plates was investigated by many authors [1-10]. However, due to the available manufacturing techniques microchannels feature more complex geometries which have been the focus of many recent works [11-22]. If a KOH-anisotropic etching technique is employed on <100> silicon wafers, it is possible to obtain microchannels having a triangular cross-section with a fixed value of aspect ratio β defined as the ratio of the altitude h and the side b (see figure 1) equal to 0.707; this value depends on the orientation of the silicon crystal planes. However, using different microfabrication techniques it is possible to obtain triangular cross sections having any aspect ratio.

Few papers have specifically addressed the issue of EOFs through triangular microchannel. Liao et al. [23] presented a numerical analysis of pure and combined pressure-driven/electro-osmotic flows inside equilateral triangular ducts. They investigated the effect of pressure gradient on the fluid behavior, concluding that the positive pressure gradient increases the mass flux of the electrolyte solution and the negative one leads to a decrease in the fluid mass flux. They also analyzed the influence of the length ratio (i.e. the product of the Debye-Hückel parameter and the characteristic channel dimension) on the fluid velocity, showing that as the length ratio increases the fluid mass flux increases as well. More recently semi-analytical solutions of EOFs in polygonal micro-ducts (i.e. equilateral triangular, square, and hexagonal cross-sections) have been derived by Wang and Chang [24] along with simple approximated correlations which enable to evaluate the net flow rate.

Despite these important contributions, a detailed analysis for electro-osmotic flows in triangular geometries is still missing. The present work is intended to numerically investigate both pure electro-osmotic and combined electro-osmotic/pressure-driven flows inside microchannels featuring a triangular cross-section. The effect of the geometric features, the electrokinetic parameters and the pressure gradient on the flow behavior is investigated. Finally, two correlations which provide the characteristic curve of the pump according to the main non-dimensional parameters, are presented.

2. Governing equations

The microchannel considered in the present study is characterized by a cross-sectional geometry that corresponds to an isosceles triangle.

For an isothermal fluid with constant properties and a laminar, fully developed flow, the equation of motion is given by the modified Navier–Stokes equation:

$$\mu \nabla^2 u(\xi, \psi) = -\rho_e(\xi, \psi) E_{ext} + \frac{dp}{d\omega} \quad (1)$$

where u and μ are the fluid velocity and dynamic viscosity, respectively. The term $\rho_e(\xi, \psi) E_{ext}$ denotes the electric force per unit volume acting on the fluid (ρ_e is the net charge distribution while E_{ext} is the applied electric field per unit length, assumed uniform over the channel cross-section); the last term on the right hand side of equation (1) is the pressure gradient along the channel.

The charge distribution can be calculated by means of the Poisson-Boltzmann equation:

$$\varepsilon \nabla^2 \phi(\xi, \psi) = -\rho_e(\xi, \psi) = -e \sum_{i=1}^N z_i n_{i\infty} \exp\left(-\frac{z_i e \phi(\xi, \psi)}{K_B T_R}\right) \quad (2)$$

ϕ being the electric potential and ε the permittivity of the solution. The second identity is a consequence of the assumption that the charge distribution is basically unperturbed from equilibrium and it is valid as long as there is no overlap of the EDL in the cross section. In the last term of equation (2) e is the magnitude of the elementary charge, z_i is the valence of the i -th ionic specie, $n_{i\infty}$ is the ionic

number concentration at the neutral state of the i -th ionic specie (of N species), K_B is the Boltzmann constant and T_R is the thermodynamic temperature, which is a known scalar quantity, since the flow is considered isothermal.

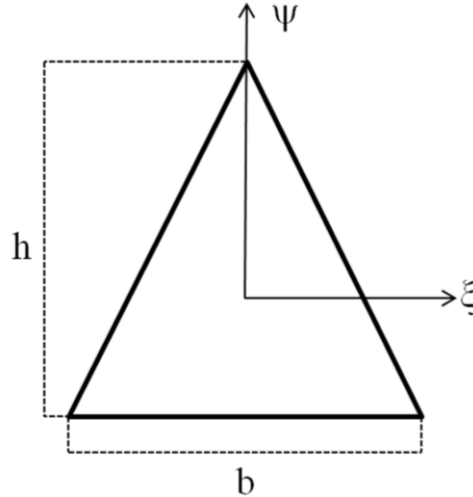


Figure 1. Microchannel cross-sectional geometry.

In a non-dimensional form, the Poisson-Boltzmann equation and the momentum equation can be rewritten as follows:

$$\nabla^2 \Phi(x, y) = D_e^2 \sinh(\Phi(x, y)) \quad (3)$$

$$\nabla^2 U(x, y) = D_e^2 \frac{(G_{EO} - \nabla^2 \Phi(x, y))}{Z} \quad (4)$$

where $\Phi = e\phi/K_B T_R$ is the dimensionless electric potential, $x = \xi/D_h$, $y = \psi/D_h$ and $z = \omega/D_h$, D_h being the hydraulic diameter, are the reduced coordinates, D_e is the electrokinetic diameter, U denotes the non-dimensional fluid velocity defined with respect to the Helmholtz-Smoluchowski velocity [16] and $Z = e\zeta/K_B T_R$ indicates the dimensionless zeta-potential, that is the electric potential at the wall.

The electrokinetic diameter D_e is the product of the Debye-Hückel parameter k and D_h , where k can be calculated by:

$$k = \left(\frac{e^2}{\epsilon k_B T} \sum_{i=1}^N z_i^2 n_{i\infty} \right)^{1/2} \quad (5)$$

The non-dimensional parameter G_{EO} denotes the ratio between pressure surface forces and electrical body forces acting on the fluid:

$$G_{EO} = \frac{\frac{dp}{d\omega}}{e E_{ext} \sum_{i=1}^N z_i^2 n_{i\infty}} \quad (6)$$

The governing equations are supplemented by the following boundary conditions:

$$\Phi|_w = Z \quad U|_w = 0 \quad (7)$$

However, due to the symmetry, the computational domain may be reduced to an half of the triangular cross-section. Therefore equations (3) and (4) are subject to the following boundary conditions on the inner edges:

$$\frac{\partial \Phi}{\partial x} \Big|_{x=0} = 0 \quad \frac{\partial U}{\partial x} \Big|_{x=0} = 0 \quad (8)$$

3. Results

The governing equations defined by equations (3) and (4) together with their boundary conditions were solved using the COMSOL MultiphysicsTM simulation environment (release 4.2a), where a non uniform mesh with an enhanced refinement in the domain of the EDL close to the walls was employed. Since the analytic solution for triangular microducts is still lacking, to validate the numerical model the results for $\beta=0.866$ (equilateral triangular) and $G_{EO}=0$ (pure electro-osmotic flow) were compared with the semi-analytical solutions for polygonal microchannels available in literature [24].

The accuracy of the solution was checked by carrying out numerical simulations with $D_e=200$ and $G_{EO}=0$ on the different grid sizes. In figure 2a the ratio between the value of the dimensionless volumetric flow rate obtained numerically for an equilateral triangle and its value computed by [24] (i.e. V_{ref}) as a function of the mesh elements (N_{el}) is presented. It is evident that for a number of elements N higher than 7314 the value of the volumetric flow rate obtained by using COMSOL becomes independent on the grid size and tends to the same value reported in [24]. Therefore, in all the numerical runs here presented a non uniform mesh characterized by at least 7314 elements was chosen.

In figure 2b, the comparison between the volumetric flow rate obtained numerically for an equilateral triangle ($\beta=0.866$) and the values obtained by Wang and Cheng [24] is shown as a function of the electro-kinetic diameter. The perfect agreement between the numerical data and the semi-analytical ones obtained in [24] can be considered a benchmark for the numerical procedure followed in this work.

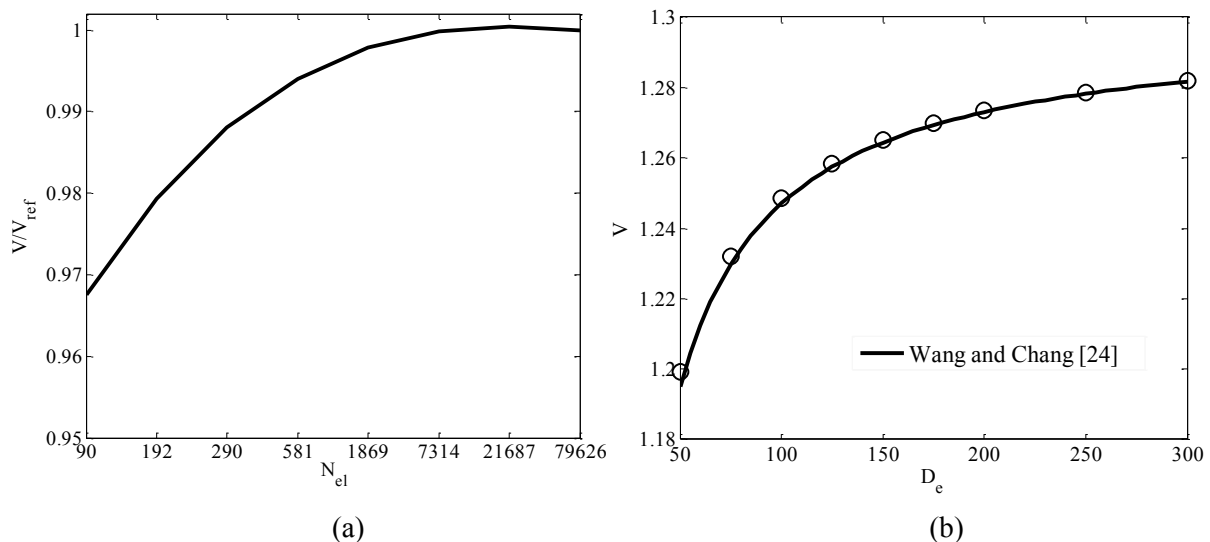


Figure 2. Equilateral triangle: (a) Mesh independence analysis; (b) Volumetric flow rate as a function of the electrokinetic diameter.

After validating the numerical procedure and checking the accuracy of the numerical solution, several simulations were performed considering different values of the aspect ratio, the electrokinetic diameter and the pressure gradient.

The results here presented were obtained by considering water as electrolyte (concentration set to 10^{-6} M) at 293 K (i.e. thermodynamic temperature T_R). The zeta potential was set to 25.275 mV and hydraulic diameter was varied between 1.9273 μm and 28.910 μm .

The effects of the opposing pressure gradient on the local velocity field are shown in figure 3 for two different values of the aspect ratio, namely $\beta=0.2$ and $\beta=0.866$ (equilateral triangle), for $D_e=100$ and $Z=1$.

When the flow is driven only by the electro-osmotic force ($G_{EO}=0$), the velocity profile is basically flat, like the ideal plug flow. If an opposing pressure gradient is applied, the velocity profile tends to get a curved shape because the flow driven by the pressure force overcomes the one induced by the electro-osmosis. Trends in figure 3 also point out that as the aspect ratio increases the influence of the opposing pressure gradient becomes less marked.

When the pressure gradient is favorable, the two flow-driving mechanisms (pressure and electric potential) act in the same direction and the velocity get markedly enhanced as the G_{EO} increases. Figure 4 shows the velocity field in such conditions for the same aspect ratios and electrokinetic diameter of fig. 3. It can be seen that the increase in velocity is more pronounced for smaller aspect ratios at any G_{EO} .

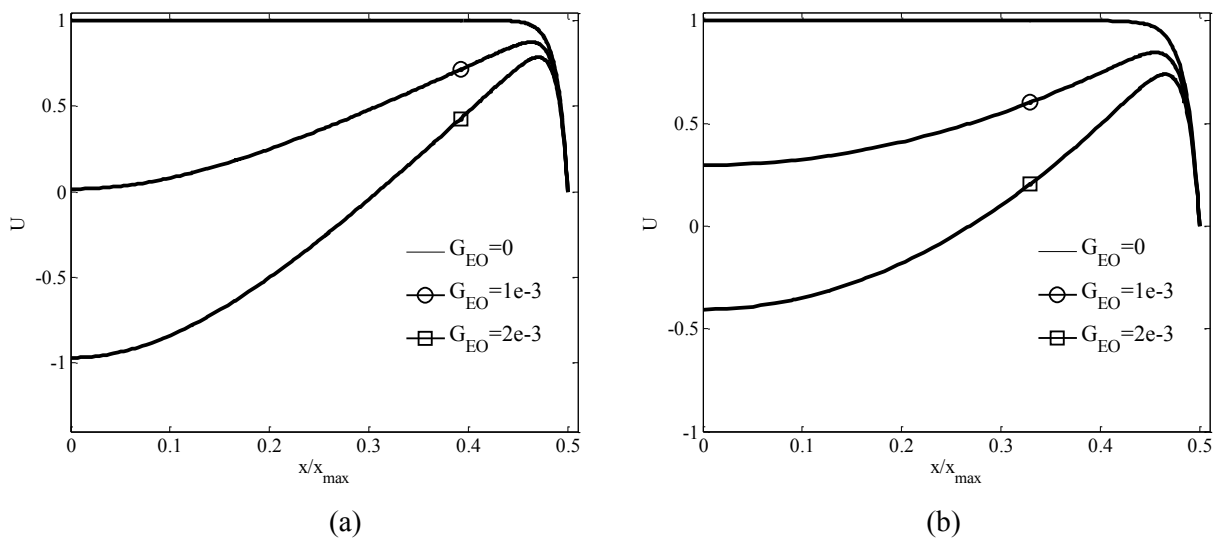


Figure 3. Velocity profiles at $y=y_{max}/2$ for positive values of G_{EO} : (a) $\beta=0.2$; (b) $\beta=0.866$ (equilateral triangle).

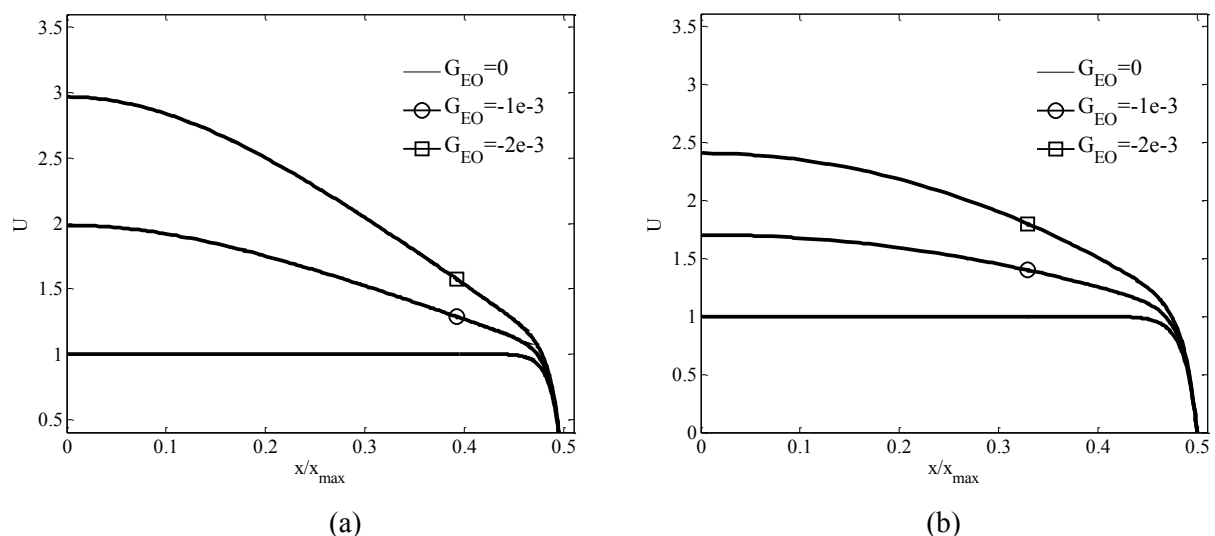


Figure 4. Velocity profiles at $y=y_{max}/2$ for negative values of G_{EO} : (a) $\beta=0.2$; (b) $\beta=0.866$ (equilateral triangle).

The effect of the aspect ratio and the electrokinetic diameter on the maximum volumetric flow rate (i.e. the volumetric flow rate for pure electro-osmotic flow) is shown in figure 5a. It can be seen that V_{max} is significantly influenced by the aspect ratio, as observed by Geri et al. [16] in rectangular and trapezoidal microchannels and by Vocale et al. [19] in elliptic microducts. However, this effect is more evident for small value of the aspect ratio while it becomes less marked for high values of β . On the other hand the electrokinetic diameter plays a less important role in determining the maximum flow rate.

When a pressure field opposes the electro-osmotic flow, the fluid velocity is reduced (figure 3). The flow rate consequently decreases too and it becomes zero when the flow due to the electro-osmosis is balanced by the flow in the opposite direction, driven by the pressure force. The value of the G_{EO} number for which the volumetric flow rate becomes zero is called critical G_{EO} [16]. $G_{EO,c}$ (i.e. critical G_{EO}) as a function of aspect ratio for different values of the electrokinetic diameter is depicted in figure 5b.

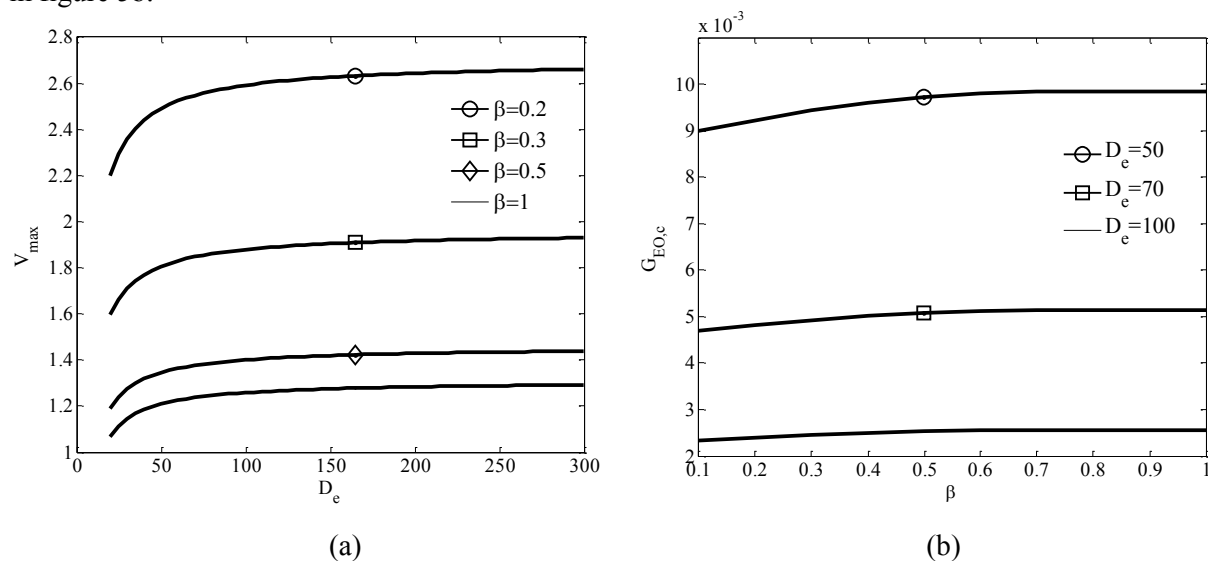


Figure 5. Influence of the aspect ratio and electrokinetic diameter on flow behavior: (a) Maximum volumetric flow rate; (b) Critical G_{EO} .

It can be seen that the critical G_{EO} is significantly influenced by the electrokinetic diameter, therefore this parameter is very important in evaluating the performance of the EOPs (electro-osmotic pumps) in terms of pressure, as it occurs in microducts characterized by different geometries [16,19].

The maximum volumetric flow rate and $G_{EO,c}$ are important because, as it has been shown [16], for a given geometry, aspect ratio and electrokinetic diameter they allow to determine the linear relationship between the flow rate and G_{EO} , i.e., the characteristic curve of the electro-osmotic pump with chosen features. Knowing the characteristic curve is very important to properly design, optimize and integrate the pump in any microfluidic device. To this end, in the literature there have been suggested a couple of correlations to estimate such values for different geometries of the micro-channel, namely for rectangular, trapezoidal and elliptical cross-sections [16,19]. For the sake of clarity, let us recall here their formulation. The maximum dimensionless volumetric flow rate is given by the following expression:

$$V_{max} = A \left(1 - \frac{\tanh \frac{D_e}{2}}{\frac{D_e}{2}} \right)^2 \quad (9)$$

being A the non-dimensional cross-sectional area.

The critical G_{EO} , as a function of the electrokinetic diameter, the aspect ratio and the non dimensional zeta potential, can be evaluated by:

$$G_{EO,c} = 48 \frac{Z}{D_e^2} \left(1 - \frac{\tanh \frac{D_e}{2}}{\frac{D_e}{2}} \right)^2 g(\beta) F(\beta) \quad (10)$$

This last correlation in particular was modified to use the same expression suggested for rectangular and trapezoidal microchannels on elliptical geometries. While equation (9) works really well also for triangular cross-sections, as shown in figure 6, the correlation for the critical G_{EO} does not. The correction factor is not enough to account for the dependence on the aspect ratio. However, since the functional dependence on the electrokinetic diameter is fully captured, a very good fitting can be achieved just by modifying the function $g(\beta)$, disregarding the area-based correction factor introduced in [19], i.e. setting $F(\beta)=1$. More specifically, it has been found that using a second order polynomial in the form:

$$g(\beta) = a_1 \beta^2 + a_2 \beta + a_3 \quad (11)$$

allows an estimation of $G_{EO,c}$ with less the 2% error compared to numerical results for triangular geometries. In table 1 the coefficients a_i are shown. Figure (7) shows the comparison between the value of $G_{EO,c}$ evaluated by the correlations (i.e. the correlation proposed in [19] and the modified correlation) and numerical for few different cases. It can be observed that the correlation proposed in the present study fits the data in a better way.

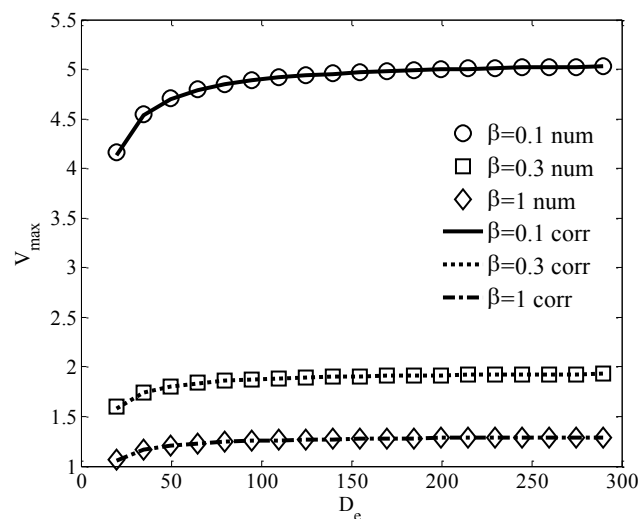


Figure 6. Comparison between the correlation for volumetric flow rate and numerical results.

By means of equations (9) and (10), it is possible to draw the characteristic curve of any electro-osmotic pump with a triangular cross-section for a given aspect ratio, electrokinetic diameter and non-dimensional zeta-potential. The determination of a different dependence on the aspect ratio for different geometries is a simple and effective engineering approach. A more general expression for the critical G_{EO} , based on physical arguments, is currently under investigation.

Table 1. Coefficients of equation (11).

a_1	a_2	a_3
-0.0959	0.1566	0.49318

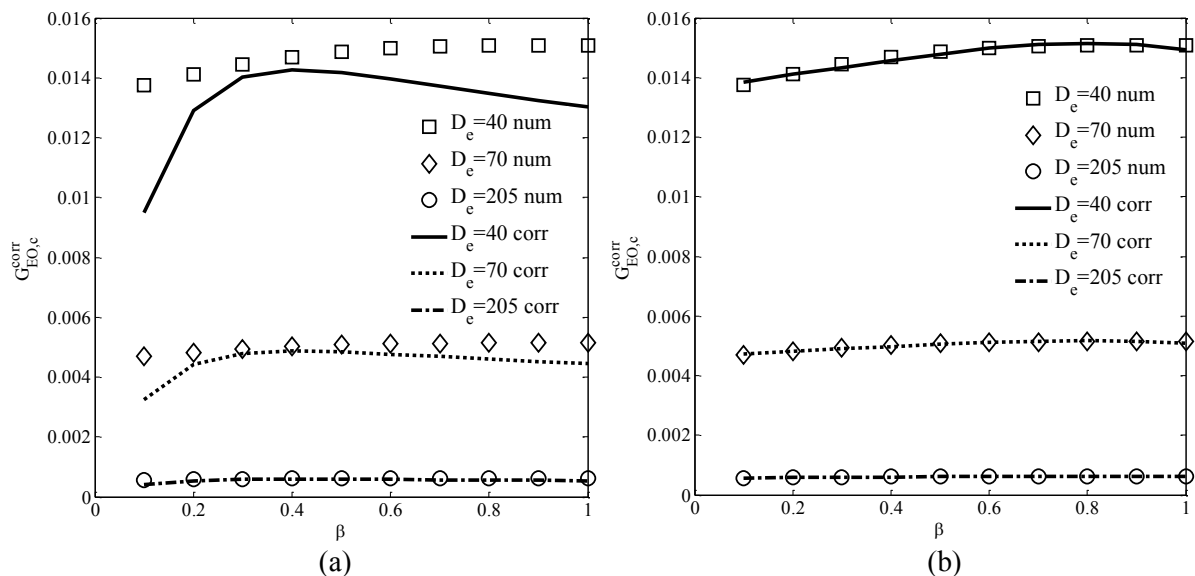


Figure 7. Comparison between the proposed correlation for critical G_{EO} and numerical results: (a) correlation proposed in [19]; (b) correlation proposed in the present study.

4. Conclusions

The dynamic behavior of electro-osmotically driven flow through triangular microchannels has been investigated. Both pure and combined electro-osmotic flows have been analyzed. The fluid has been considered isothermal and with constant properties, undergoing a laminar fully developed flow. The Poisson-Boltzmann equation and the modified Navier-Stokes equation have been solved using COMSOL MultiphysicsTM. Numerical results have been obtained for different values of the main parameters that characterize the behavior of electro-osmotic flows.

The results point out that both the aspect ratio β of the cross-section and the electrokinetic diameter D_e significantly influence the velocity field. The maximum volumetric flow rate strongly depends on the value of β , while D_e is crucial in the determination of the maximum pressure that can be overcome by the EOF, here represented by the dimensionless number $G_{EO,c}$.

Finally, two correlations available in the literature for the maximum volumetric flow rate and the critical G_{EO} have been tested against the numerical results. While the functional dependence of the flow rate seems to be already well understood, the dependence of the G_{EO} on the aspect ratio is still theoretically undetermined since the available functions and correction factors do not work for every geometry. In order to get $G_{EO,c}$ in microchannels characterized by triangular geometries, a new expression for the functional dependence on the aspect ratio has been derived using the numerical results. This way, the maximum volumetric flow rate and the critical G_{EO} can be estimated with an error smaller than 2% under a wide range of operative conditions. Characteristic curves of electro-osmotic pumps featuring triangular cross-sectional geometry are therefore available through simple analytical correlations that involve only three fitting coefficients.

Acknowledgments

This work has been carried out thanks to the financial support of the PRIN2009TSYPM7_001 project “Single-phase and two-phase heat transfer for microtechnologies. Heat transfer and fluid flow in microscale”.

References

- [1] Burgreen D and Nakache F R 1964 *J. Physical Chemistry* **68** 1084–91

- [2] Rice C L and Whitehead R 1965 *J. Physical Chemistry* **69** 4017–24
- [3] Sørensen T S and Koefoed J 1974 *J. Chem. Soc. Faraday Trans II* **70** 665–75
- [4] Qian Y, Yang G and Bowen W R 1997 *J. Colloid Interface Sciences* **190** 55-60
- [5] Mala G M, Li D and Dale J D 1997 *Int. J. Heat Mass Transfer* **40** 3079-88
- [6] Mala G M, Li D, Werner C, Jacobasch H J and Ning Y B 1998 *Int. J. Heat Fluid Flow* **18** 489-96
- [7] Dutta P and Beskok A 2001 *Analytical Chemistry* **73** 5097-5102
- [8] Chen C H and Santiago J G 2002 *J. Microelectromechanical Systems* **11** 672-83
- [9] Zhao C, Zholkovskij E, Masliyah J and Yang C J. 2008 *Colloid Interface Science* **326** 503-510
- [10] Jamaati J, Niazmand H and Renksizbulut M 2010 *Int. J. Thermal Sciences* **49** 1165-1174
- [11] Yang C and Li D 1997 *J. Colloid Interface Sciences* **194** 95-107
- [12] Yang C, Li D and Masliyah J H 1998 *Int. J. Heat Mass Transfer* **41** 4229-49
- [13] Mala G M, Yang C and Li D 1998 *Colloids Surface A* **135** 109-16
- [14] Yang C and Li D 1998 *Colloids Surface A* **143** 339-53
- [15] Arulanandam S and Li D 2000 *Colloid Surface A* **161** 89-102
- [16] Geri M, Lorenzini M and Morini G L 2012 *Int. J. Thermal Sciences* **55** 114-21
- [17] Horiuchi K, Dutta P and Richards C D 2007 *Microfluidics and Nanofluidics* **3** 347–358
- [18] Hsu J P, Kao C Y, Tseng S and Chen C J 2002 *J. Colloid Interface Sciences* **248** 176-84
- [19] Vocale P, Geri M, Cattani L, Morini G L and Spiga M 2013 *La Houille Blanche – Int. J. Water* **3** 42-49
- [20] Vocale P, Geri M, Cattani L, Morini G L and Spiga M 2013 *Int. J. Thermal Sciences* **72** 92-101
- [21] Xuan X and Li D 2005 *J. Colloid Interface Science* **289** 291-303
- [22] Goswami P and Chakraborty S 2011 *Microfluidics and Nanofluidics* **11** 255–267
- [23] Liao Q, Wen T Y and Zhu X 2008 *Applied Thermal Engineering* **28** 1463-70
- [24] Wang C Y and Chang C C 2011 *Electrophoresis* **32** 1268–72